

# Properties of Ternary Insulating Systems: The Electronic Structure of $\text{MgSO}_4\cdot\text{H}_2\text{O}$

V. V. Maslyuk,\* C. Tegenkamp,† and H. Pfnür

*Institut für Festkörperphysik, Universität Hannover, Appelstr. 2, 30167 Hannover, Germany*

T. Bredow

*Theoretische Chemie, Universität Hannover, Am Kleinen Felde 30, 30167 Hannover, Germany*

*Received: November 18, 2004; In Final Form: February 15, 2005*

Structural and electronic properties of (100)-oriented  $\text{MgSO}_4$  and  $\text{MgSO}_4\cdot\text{H}_2\text{O}$  surfaces and the adsorption of water on the latter were investigated theoretically with a combination of ab initio and semiempirical methods. Ab initio electronic structure calculations were based on a density functional theory (DFT)–Hartree-Fock (HF) hybrid approach. The semiempirical method MSINDO was used for the determination of the local adsorption geometry of the water molecule. With the hybrid method good agreement was obtained with the experimental band gap of 7.4 eV determined with electron energy loss spectroscopy of polycrystalline  $\text{MgSO}_4\cdot\text{H}_2\text{O}$  samples under ultrahigh vacuum conditions. The valence bands of the (100) surfaces of both  $\text{MgSO}_4$  and  $\text{MgSO}_4\cdot\text{H}_2\text{O}$  are formed mainly by the O2p levels, whereas the S2p states contribute to the lower part of the conduction band. The preferred adsorption site of water at  $\text{MgSO}_4\cdot\text{H}_2\text{O}$  (100) is above a surface Mg atom. The water molecule is stabilized by two additional hydrogen bonds with surface atoms. Only small differences between the electronic structure of  $\text{MgSO}_4\cdot\text{H}_2\text{O}$  and  $\text{MgSO}_4$  were observed. Also, the molecular adsorption of water on the  $\text{MgSO}_4\cdot\text{H}_2\text{O}$  surface leads to only small shifts of the electronic energy levels.

## I. Introduction

The electronic properties of crystalline insulators and of their surfaces have been in the focus of various investigations both theoretically<sup>1</sup> and experimentally.<sup>2–4</sup> The motivation for these investigations is not only the need to clarify the role of insulating support materials in context with their activity in heterogeneous catalysis but also the role of various kinds of defects as chemically active sites and their relevance as pinning centers in nanostructuring. Usually insulating surfaces can promote certain chemical reactions only after the generation of defects or after the deposition of metal clusters.<sup>1</sup> However, also the shape and size of the clusters is determined by the detailed atomic structure of the surface and the energetic interplay between the metal and the insulating surface, which, of course, defines the yield of such catalytic reactions. Within this context, especially binary insulators with two different kinds of atoms have been investigated intensely in the past.<sup>1</sup>

Studies on ternary systems like  $\text{MgSO}_4$  have not been in the focus of the research so far, because experimentally it is still difficult to grow single crystals and prepare their surfaces with sufficient perfectness. Simulations of such materials, on the other hand, have to cope with problems of comparatively large unit cells with many atoms and with the rather low symmetry of most systems. This makes them interesting candidates for comparisons of ab initio and more approximate semiempirical methods.

Incorporating water into the crystalline structure of magnesium sulfate gives kieserite ( $\text{MgSO}_4\cdot\text{H}_2\text{O}$ ), which, for instance, is used in agriculture for manuring.<sup>5</sup> Kieserite exists naturally as a mineral, which is in general mixed with other minerals

such as halite (NaCl) and silvite (KCl). By addition of conditioner molecules, which adsorb on the surfaces of the minerals, and after appropriate mechanical treatment, these minerals can be separated electrostatically, making also adsorption processes and the adsorption induced electronic states an interesting subject of investigation.<sup>6</sup>

This paper presents first results on the geometric and electronic structure of bulk  $\text{MgSO}_4$  and  $\text{MgSO}_4\cdot\text{H}_2\text{O}$  with emphasis on simulations and their methodology. The comparison of ab initio and semiempirical methods with experimental data is meant as a test of the reliability of the various methods and to form a basis for semiempirical calculations, which allow the investigation of much larger systems. Starting with the  $\text{MgSO}_4$  system, we extended our calculations to the (100)-oriented surface of kieserite and investigated in a third step the adsorption of water at different sites on this surface.

## II. Computational Methods and Experimental Setup

**A. Computational Methods.** Two different theoretical methods were used to calculate the properties of  $\text{MgSO}_4$  and  $\text{MgSO}_4\cdot\text{H}_2\text{O}$ . Their electronic structure was calculated with the DFT–HF hybrid approach PWIPW.<sup>7</sup> In this method the exchange functional is a linear combination of the HF expression (20%) and the Perdew-Wang generalized-gradient functional (PWGGA).<sup>8</sup> Electron correlation is included by the PWGGA correlation functional. This approach describes the electronic structure of insulating oxides in reasonable agreement with experiment, as has been shown for MgO, NiO and CoO.<sup>7</sup>

The periodic ab initio calculations were performed using the crystalline orbital program CRYSTAL03.<sup>9</sup> The Bloch functions are expanded as a linear combination of Gaussian-type atomic orbitals. The reliability of the computed results depends on the choice of the atomic basis sets. Therefore, those basis sets for

\* Corresponding author. Present address: Halle-Wittenberg, Von-Seckendorff-Platz 1, 06099 Halle. E-mail: volodymyr@physik.uni-halle.de

† E-mail: tegegenkamp@fkp.uni-hannover.de

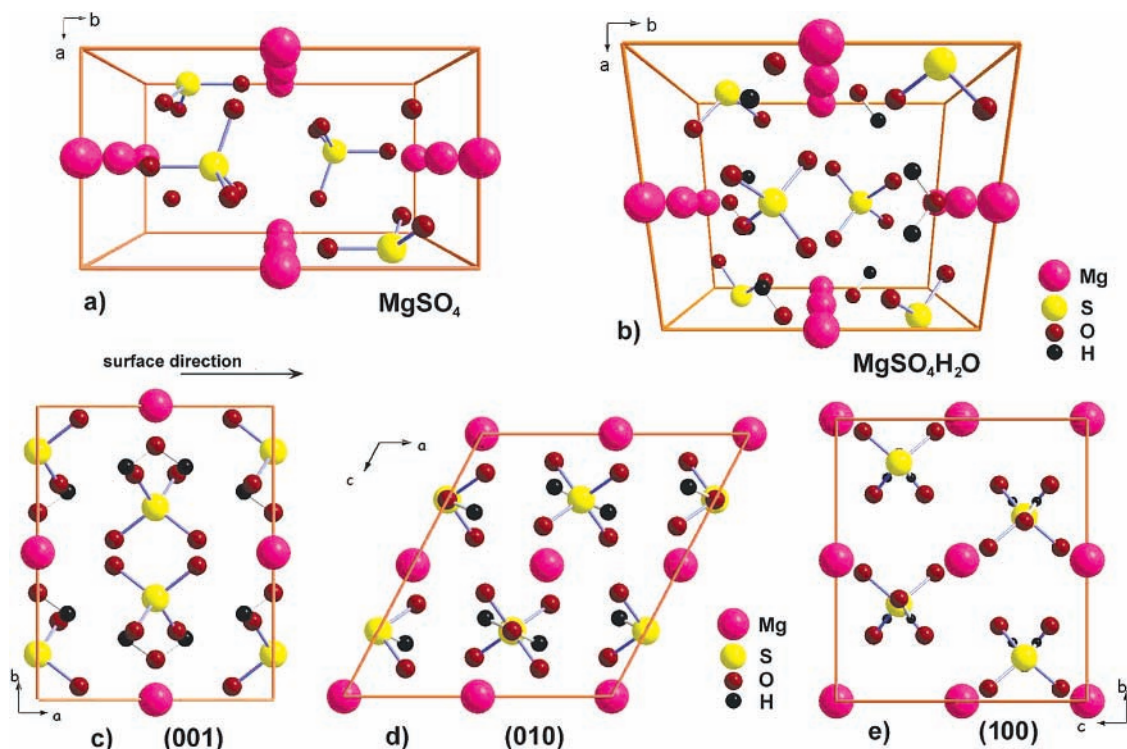


**Figure 1.** Crystal structures of bulk MgSO<sub>4</sub> (a) and MgSO<sub>4</sub>·H<sub>2</sub>O (b). In the lower part projections of the atomic positions in MgSO<sub>4</sub>·H<sub>2</sub>O onto the (001) (c), (010) (d) and (100) planes (e) are shown.

Mg, S, and O were used that have been optimized in previous CRYSTAL studies. The 8-511G\* and 8-411G\* basis sets for Mg and O, respectively, have been derived for MgO<sup>10</sup>, which is expected to be a reasonable choice for the present systems. For sulfur, an 86-311G\* basis set was chosen, where the outer sp and d exponents have been optimized for CaSO<sub>4</sub>.<sup>11</sup> The description of the O and H atoms in water was realized with the standard basis set 6-31G\*.<sup>12</sup> We also investigated the effect of additional diffuse and polarization functions on the calculated band gap of bulk MgSO<sub>4</sub>·H<sub>2</sub>O and the (100) surface of MgSO<sub>4</sub>·H<sub>2</sub>O, and on energetic properties.

For sampling in reciprocal space, shrinking factors  $s$  of 4 were used in the Monkhorst net.<sup>13</sup> This leads to a total number of 21  $k$  points in the first Brillouin zone of MgSO<sub>4</sub> and of 24  $k$  points for MgSO<sub>4</sub>·H<sub>2</sub>O.

CRYSTAL03 allows the optimization of internal coordinates of three- and two-dimensional systems using analytical gradients and an updated Hessian approach.<sup>9</sup> Lattice parameters must be optimized numerically. The optimization of adsorbate structures is, however, very time-consuming with CRYSTAL03. For this reason the semiempirical SCF MO method MSINDO<sup>14</sup> was employed for the study of water adsorption on the MgSO<sub>4</sub>·H<sub>2</sub>O (100) surface. Both the orientation of the water molecule and the atomic positions of the surface were optimized in these simulations. The so obtained atomic coordinates were used for subsequent analyses of the electronic structure with CRYSTAL03 PW1PW.

MSINDO is a modification of the previous version SINDO1.<sup>15</sup> An approximate Löwdin orthogonalization of the valence orbitals is performed. Inner orbitals are taken into account by Zerner's pseudopotential.<sup>16</sup> More details about the methods can be found elsewhere.<sup>17,18</sup> Due to its computational efficiency the MSINDO method allows to simulate much larger and therefore more realistic model systems compared to first-principles methods, e.g., the adsorption of water on the MgSO<sub>4</sub>·H<sub>2</sub>O surface.

MSINDO surface simulations were performed with the recently implemented cyclic cluster model (CCM).<sup>19,20</sup> In this model periodic boundary conditions are directly applied to a cluster of a moderate size. A CCM calculation is similar to a supercell calculation at the  $\Gamma$  point  $k = 0$  but with an interaction region that is defined by the cluster geometry and not by cutoff thresholds. A comparison of the supercell approach and the CCM was given recently.<sup>21</sup>

**B. Experimental Setup.** The experiments were carried out in a vacuum chamber at a base pressure of  $10^{-8}$  Pa. As substrates we used naturally grown, polycrystalline MgSO<sub>4</sub>·H<sub>2</sub>O minerals, which were brought inside the chamber by a load lock system. To characterize the electronic structure of the surface, photoelectron spectroscopy (UPS and XPS) and electron energy loss spectroscopy (EELS) measurements have been performed. A more detailed description of the vacuum system is described elsewhere.<sup>6</sup> The charging of MgSO<sub>4</sub>·H<sub>2</sub>O during the UPS measurements leads to a strong broadening and shifting of all emissions. The charging during the electron energy loss spectroscopy (EELS) was less pronounced, i.e., the full width at half-maximum of the elastic peak was around 0.5 eV.

### III. Crystallographic Parameters and Structural Relaxations

The orthorhombic, basis-centered structure of MgSO<sub>4</sub> (space group  $D_{2h}^{17} - Cmcm^{22}$ ) is shown in Figure 1a. The SO<sub>4</sub> tetrahedrons are centrosymmetrically arranged around the Mg atoms. Therefore, the unit cell of MgSO<sub>4</sub> contains four formula units (4 Mg atoms, 4 S atoms and 16 O atoms). The Mg atoms are located at (0,0,0); (0,0,1/2); (1/2,1/2,0); (1/2,1/2,1/2) in units of the lattice vectors, and the S atom positions are (0, $\delta$ ,1/2); (0, $\delta$ ,3/4); (1/2,1/2+ $\delta$ ,1/4); (1/2,1/2- $\delta$ ,3/4) with  $\delta = 0.37$ , as revealed by X-ray experiments.<sup>22</sup> The O atoms are forming almost regular tetrahedra around the sulfur atoms. However, the small distortion of the SO<sub>4</sub> units defines two different kinds

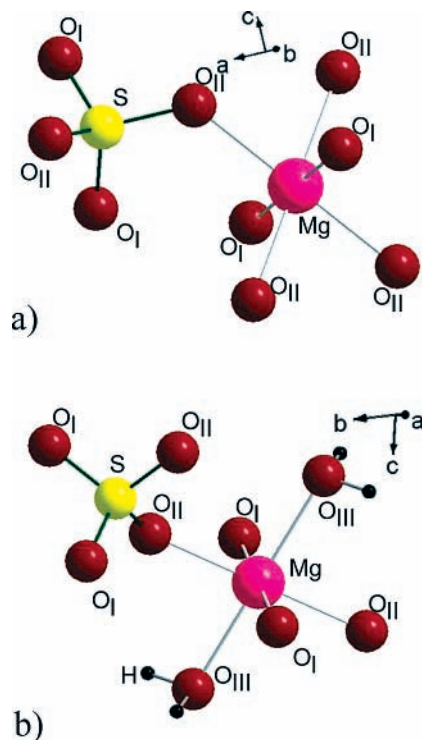


**Figure 2.** Representative  $\text{MgSO}_4$  (a) and  $\text{MgSO}_4 \cdot \text{H}_2\text{O}$  (b) structure units with relevant bond lengths (cf. Table 1).

**TABLE 1: Comparison of Calculated and Experimental Lattice Vectors and Bond Distances ( $\text{\AA}$ , degrees) of Crystalline  $\text{MgSO}_4$ , and  $\text{MgSO}_4 \cdot \text{H}_2\text{O}$ <sup>a</sup>**

system	parameter	exp. <sup>22,23</sup>	PW1PW	MSINDO
$\text{MgSO}_4$	lattice vectors			
	$a$	5.18	5.19	5.01
	$b$	7.89	7.89	7.89
	$c$	6.51	6.50	6.47
	bonds			
	$\text{S}-\text{O}_I$	1.557	1.466	1.458
$\text{S}-\text{O}_{II}$	1.517	1.515	1.459	
$\text{Mg}-\text{O}_I$	2.011	2.014	2.018	
$\text{Mg}-\text{O}_{II}$	2.093	2.114	2.105	
$\text{MgSO}_4 \cdot \text{H}_2\text{O}$	lattice vectors			
	$a$	6.89	6.90	6.88
	$b$	7.62	7.63	7.50
	$c$	7.65	7.63	7.64
	$\beta$	117.7	117.6	117.6
	bonds			
	$\text{S}-\text{O}_I$	1.465	1.447	1.450
	$\text{S}-\text{O}_{II}$	1.468	1.498	1.457
	$\text{Mg}-\text{O}_I$	2.022	2.035	2.003
	$\text{Mg}-\text{O}_{II}$	2.045	2.040	2.006
	$\text{Mg}-\text{O}_{III}$	2.177	2.168	2.181
$\text{O}_{III}-\text{H}$	0.938	1.001	0.974	

<sup>a</sup> The corresponding bonds for the bulk materials are shown in Figure 2.

of O groups, which can be distinguished by different S–O bond lengths, S–O<sub>I</sub> and S–O<sub>II</sub> (Figure 2). The Mg atoms themselves are surrounded by 6 nearest neighbor O atoms, forming distorted MgO<sub>6</sub> octahedra with two different Mg–O bond lengths, denoted as Mg–O<sub>I</sub> and Mg–O<sub>II</sub> (Figure 2). The optimized lattice parameters  $a$ ,  $b$ , and  $c$  and the corresponding bond lengths as obtained with CRYSTAL PW1PW and MSINDO are shown in Table 1 and compared to available experimental results.

Kieserite ( $\text{MgSO}_4 \cdot \text{H}_2\text{O}$ ) is chemically formed by incorporating one water molecule per  $\text{MgSO}_4$  unit. This leads to further reduction of the symmetry of the sulfate crystal, i.e.,  $\text{MgSO}_4 \cdot \text{H}_2\text{O}$  has a monoclinic structure ( $C_{2h}^6$ ) (cf. Figure 1b).<sup>23</sup> For better visibility, projections of the bulk structure onto the (001),

(010), and (100) planes are shown in Figure 1c,d,e. Along the [100] direction, the kieserite crystal has a layered structure with a spacing of approximately 1  $\text{\AA}$  between the closed-packed layers as indicated in Figure 1c. A cut along (100) in this region will not lead to S–O or Mg–O bond cleavage. It is therefore energetically favored over other possible cuts for the (100) surface. Each slab consists of 7 atomic layers and contains 18 atoms per primitive unit cell. In comparison to the sulfate system, the chemically bound water induces a rotation of the SO<sub>4</sub> units (30° see Figure 1). Due to this transformation, the Mg atom of kieserite has in contrast to  $\text{MgSO}_4$  three different O bonds, Mg–O<sub>I</sub>, Mg–O<sub>II</sub>, and Mg–O<sub>III</sub>, as shown in Figure 2. The third species O<sub>III</sub> is defined by the crystalline water.

Full optimization of the bulk lattice parameters and atomic coordinates was performed with the CRYSTAL package by exploiting the new feature of analytic energy gradients.<sup>9</sup> First, a full optimization of all atomic fractional coordinates was performed with lattice vectors fixed at the experimental values.<sup>22,23</sup> Starting from the obtained internal coordinates, the lengths and angles of the lattice vectors were optimized. This procedure was repeated iteratively until the forces were smaller than 0.02 eV/ $\text{\AA}$ . Similar optimizations were performed with MSINDO CCM using cyclic clusters  $\text{Mg}_{32}\text{S}_{32}\text{O}_{128}$  and  $\text{Mg}_{32}\text{S}_{32}\text{O}_{160}\text{H}_{64}$ , corresponding to  $2 \times 2 \times 2$  supercells. The optimized structure parameters obtained by the two different methods are summarized in Table 1 for  $\text{MgSO}_4$  and  $\text{MgSO}_4 \cdot \text{H}_2\text{O}$ .

Particularly, the results of the PW1PW method show a good agreement with the experimental data. The differences do not exceed 0.02  $\text{\AA}$  and 0.1° for the lattice parameters for both kieserite and magnesium sulfate. The lattice parameters obtained with MSINDO are similar except for  $a$  ( $\text{MgSO}_4$ ) and  $b$  ( $\text{MgSO}_4 \cdot \text{H}_2\text{O}$ ) where the deviations are larger than 0.1  $\text{\AA}$  (Table 1). For  $\text{MgSO}_4$  this effect is due to an underestimation of the S–O<sub>I</sub> bond length by  $\approx 0.1$   $\text{\AA}$ , while for kieserite this is not observed. Here it is more likely that the error of the lattice parameter is due to an underestimation of bond angles. The DFT–HF hybrid method PW1PW in general gives bond lengths in close agreement with experiment with deviations smaller than 0.03  $\text{\AA}$ . An exception is the O<sub>III</sub>–H bond length where the difference to the experimental value is with 0.06  $\text{\AA}$  larger than the MSINDO error (0.04  $\text{\AA}$ ). Besides the few cases mentioned above MSINDO describes the bond lengths of  $\text{MgSO}_4$  and  $\text{MgSO}_4 \cdot \text{H}_2\text{O}$  with comparable accuracy as PW1PW. For this reason no refinement of the empirical parameters for the present study was performed and the standard parameters<sup>14</sup> were used for the surface structure optimizations described below.

For comparison with adsorption experiments, the (100) surface of  $\text{MgSO}_4 \cdot \text{H}_2\text{O}$  (Figure 1e) has been studied in more detail. Other surface configurations have not been investigated in detail. Different from other low-index surfaces, e.g. (001) and (010), the electrostatic dipoles between the Mg<sup>2+</sup> ions and the SO<sub>4</sub><sup>2-</sup> units are almost within the plane for the (100) surface. For this reason the surface energy of this surface is expected to be lower than for the other planes. Furthermore, cutting the  $\text{MgSO}_4 \cdot \text{H}_2\text{O}$  bulk material in any other direction than (100) requires the cleavage of S–O or Mg–O bonds. Only for the (100)-oriented surface a superimposed layered structure can be seen, as discussed in a previous section.

In the following we will call one stoichiometric unit consisting of 7 atomic layers a superlayer. In Figure 3 the single layers are indicated by dashed lines.

In preliminary MSINDO calculations the energy required for the removal of one chemically bound water molecule out of



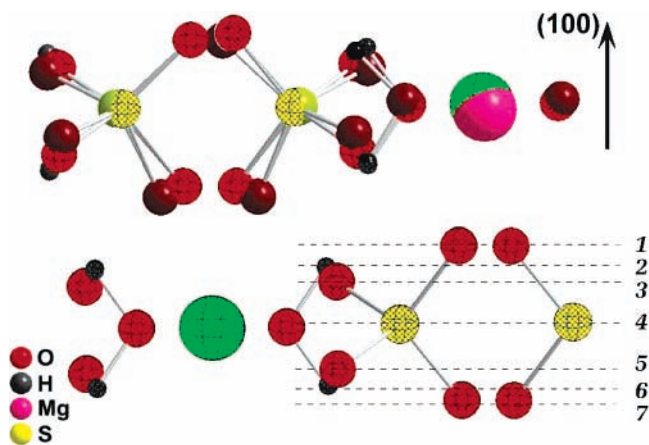


**Figure 3.** Side view of the unrelaxed and relaxed  $\text{MgSO}_4 \cdot \text{H}_2\text{O}$  (100) surface. Full circles represent the atoms of the relaxed surface and shaded circles correspond to the atomic positions of the bulk crystal. The absolute values of atomic displacements are shown in Table 2. The atomic layers are indicated by dashed lines.

**TABLE 2: Displacement  $\Delta$  (Å) of Atoms in the Kieserite (100) Surface with Respect to the Optimized Bulk Positions<sup>a</sup>**

surface atom	PWIPW	MSINDO
Mg	0.10	0.10
S	0.07	0.07
O <sub>I</sub> /O <sub>II</sub>	0.14–0.31	0.17–0.35
O <sub>III</sub>	0.05–0.22	0.05–0.24

<sup>a</sup> Comparison of PWIPW CRYSTAL and MSINDO CCM results. For the O<sub>I</sub> and O<sub>II</sub> atoms around the S atom and the O<sub>III</sub> atom of the water the minimal and the maximal displacement values are listed (see also Figure 3).

the kieserite (100) surface was calculated as 4.5 eV. Therefore, the calculations regarding the water adsorption have been performed on the perfectly stoichiometric (100)-oriented surface.

The surface was modeled by two-dimensional slab models consisting of 14 atomic layers in *a* direction (2 superlayers). Again, both the ab initio and the semiempirical methods have been used to optimize the geometry of this surface. In these optimizations both superlayers were allowed to relax. The change of the atomic positions in the (100) surface with respect to their bulk coordinates are given in Table 2. A corresponding visualization of the relaxation is shown in Figure 3.

The displacements obtained from PWIPW and MSINDO are very similar. The Mg atoms relax toward the bulk by about 0.10 Å, whereas the S atoms relax only within the (100) plane.

To maintain the O–S–O bond angles close to the optimal values, the  $\text{SO}_4$  unit rotates, so that the outermost O atoms at the surface relax toward the bulk. This reduces the effective spacing between the superlayers by approximately 0.1 Å. It is obvious that the electrostatic attraction between Mg cations and O anions is increased and the surface energy is lowered by this relaxation mechanism. It was found that the displacements of atoms in the second layer are an order of magnitude smaller than those of the outermost layers. To reduce computational effort, only atoms of the first superlayer were allowed to relax in the study of water adsorption (see below).

The atomic displacements obtained for  $\text{MgSO}_4 \cdot \text{H}_2\text{O}$  (100) are within the range of other insulating surfaces, e.g., NaCl(100) and KCl(100).<sup>24</sup>

A second verification of MSINDO was done by the comparison of the total energies obtained with the hybrid PWIPW method, but with different geometries as input data. The difference of the total energies for two relaxed surfaces (with ab initio and semiempirical methods) is small (0.32 eV). This finally demonstrates that MSINDO is a good approach for the calculation of the geometry and binding energies. Therefore, this method was extended toward the calculation of water adsorbed on  $\text{MgSO}_4 \cdot \text{H}_2\text{O}$  surface (see section V).

#### IV. Electronic Properties

The electronic structure of  $\text{MgSO}_4 \cdot \text{H}_2\text{O}$  was computed with PWIPW CRYSTAL along the high-symmetry points of the Brillouin zone,<sup>25</sup> namely  $Y \rightarrow M \rightarrow L \rightarrow A \rightarrow \Gamma \rightarrow V$ . The upper part of the valence band and the lower part of the conduction band of the bulk is shown in the left part of Figure 4. The crystal is a wide band gap insulator with a gap of 7.77 eV at the  $\Gamma$ -point. The top of the valence band has a small dispersion indicating large hole effective mass, which is often found for wide band gap insulators. The bottom of the conduction band has, however, a significant dispersion near the  $\Gamma$  point.

The calculation of band gaps, i.e., the determination of the lowest energy of the conduction band, is the most difficult part for many quantum chemical theories. The hybrid method PWIPW was originally designed to reproduce experimental band gaps, lattice parameters and thermodynamical properties of oxides.<sup>7</sup> The linear combination of HF exchange and the PWGGA exchange functional leads to a partial error cancellation and the one-particle energies provide a reasonable approximation to measured electronic spectra. For the  $\text{MgSO}_4 \cdot \text{H}_2\text{O}$  (100)

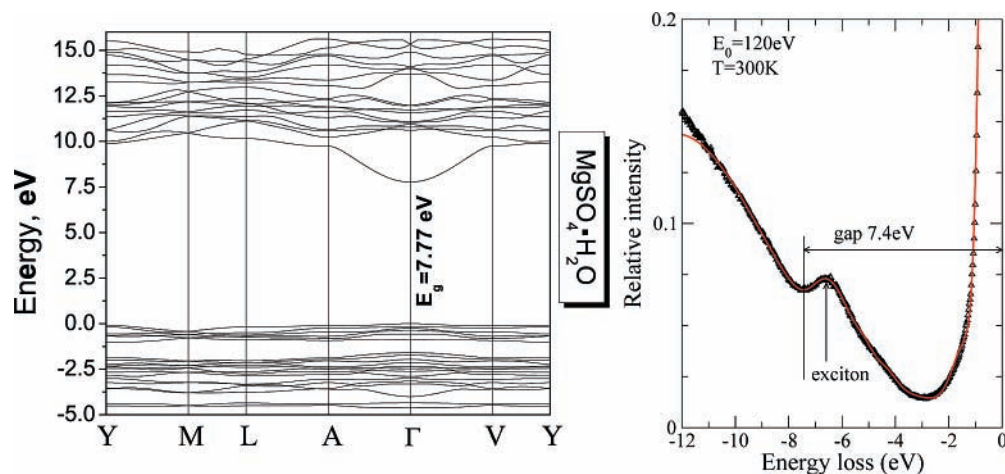


**Figure 4.** Left:  $E(k)$  dispersion relation along the  $k$  points with the highest symmetry calculated for  $\text{MgSO}_4 \cdot \text{H}_2\text{O}$ . Right: EEL-spectrum of polycrystalline kieserite. For details see text.

surface the band gap was determined to be around 7.35 eV (see below). This is in excellent agreement with results of our EELS experiments, shown in the right part of Figure 4. For these experiments polycrystalline kieserite material has been used. Due to the surface sensitivity given by the energy of the incident electron beam and due to the geometry, i.e., detection of the losses around the specularly reflected beam, mainly the excitation of an electron at the  $\Gamma$ -point is measured. However, in the EEL spectra an additional loss around 6.5 eV is found. According to other wide band gap insulators the loss can be attributed to an excitonic state of  $\text{MgSO}_4 \cdot \text{H}_2\text{O}$ . Nevertheless, as seen by experiments of water adsorption on  $\text{NaCl}(100)$  and  $\text{KCl}(100)$  surfaces, defects in form of color centers can dissociate  $\text{H}_2\text{O}$  molecules, resulting in the formation of OH centers at the surface, which show characteristic losses ( $4\sigma \rightarrow 1\pi$  transition) in the same energy range.<sup>26</sup> Therefore, to exclude similarities with adsorbed or dissociated water, the kieserite crystal was degassed for days at 400 K, i.e., below a temperature, where desorption of the chemically bound water or even a chemical decomposition of the crystal can be excluded. Also bombardment experiments with electrons (energy 100 eV) have been performed. This is a well-known technique to generate new active sites for water dissociation, but no significant changes in the emission spectra have been detected, so that we assign the loss at 6.5 eV to an excitonic state, which is not considered within the theoretical calculations.

Furthermore, the projected density of states (PDOS) of kieserite (100) was calculated to identify the individual contributions of the single atoms to the total DOS, because this is of importance for later discussions about the adsorption of water (see below) and organic molecules.<sup>27</sup> The DOS was calculated with PW1PW using the Fourier-Legendre technique<sup>28</sup> with a refined Monkhorst net using shrinking factors of 8. The projection onto atomic orbitals was based on a Mulliken analysis of the crystalline orbitals. The calculated DOS of the  $\text{MgSO}_4 \cdot \text{H}_2\text{O}$  crystal is shown in Figure 5a. The analysis of the PDOS shows that every atom has a major contribution only in one band. The Mg atoms have only very small contributions to the upper part of the valence band. Obviously, the oxidation state of the Mg atoms of both  $\text{MgSO}_4$  and  $\text{MgSO}_4 \cdot \text{H}_2\text{O}$  is close to  $\text{Mg}^{2+}$ , i.e., the interaction between Mg and the  $\text{SO}_4$  is mainly electrostatic. The lower part of the conduction band is mainly formed by unoccupied 3p states of the sulfur atoms. The Mg 3s orbitals give only small contributions to the conduction band of the crystal. This is different from  $\text{MgO}$  bulk or the  $\text{MgO}(100)$  surface.<sup>29,30</sup> The upper part of the valence band is formed by the 2p orbitals of the O atoms  $\text{O}_I$  and  $\text{O}_{II}$  from the  $\text{SO}_4$  units. The occupied states of the  $\text{H}_2\text{O}$  molecule ( $1b_1$  state) are located 4 eV below the top of the valence band.

In part (b) of Figure 5 the DOS of bulk  $\text{MgSO}_4$  is shown, calculated in a way similar as for kieserite. The origin and the structure of the density of states are the same as for the kieserite bulk material. The  $\text{MgSO}_4$  shows some additional relaxation effects, i.e., the band gap is slightly larger than for the kieserite bulk structure, but again, only the O atoms of the sulfur complexes contribute to the valence band. A comparison of the DOS of  $\text{MgSO}_4$  and  $\text{MgSO}_4 \cdot \text{H}_2\text{O}$  crystals shows that the crystal water changes the electronic structure of the  $\text{MgSO}_4$  crystal very little but still is responsible for structural changes (in our case rotating of the  $\text{SO}_4$  group and increasing of the volume).

More significant changes in the DOS are obtained when the kieserite surface is considered (cf. Figure 5c), which is probably the result of the surface relaxation. In general, the origin of the individual features in the band structure can be related to the

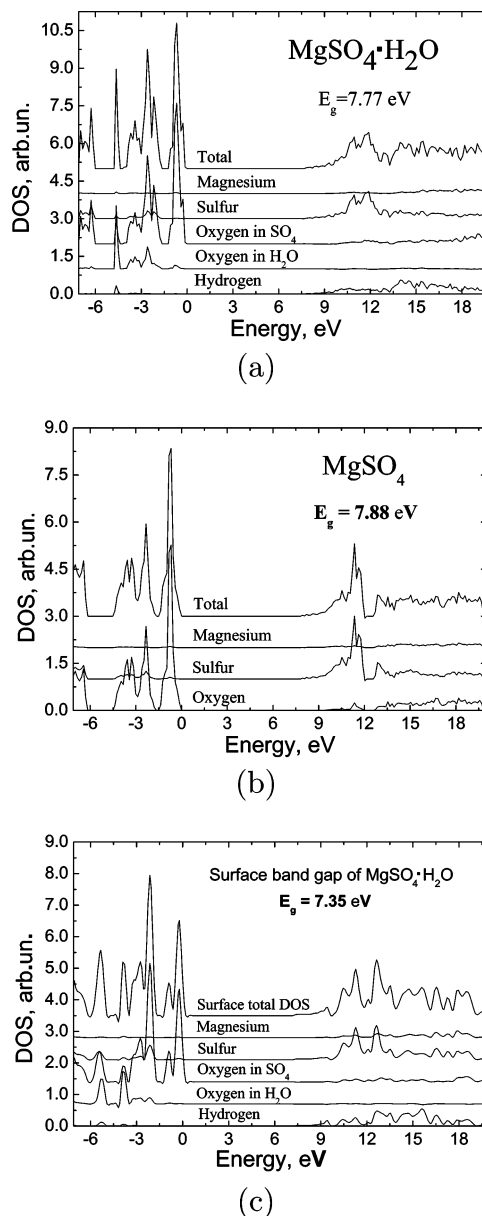


**Figure 5.** Contributions of the single atoms to the total density of states (DOS) for bulk  $\text{MgSO}_4 \cdot \text{H}_2\text{O}$  (a), bulk  $\text{MgSO}_4$  (b), and for the surface of  $\text{MgSO}_4 \cdot \text{H}_2\text{O}$  (100) (c).

same atoms as for the bulk material. Nevertheless, the relaxation of the layers near the surface is manifested by a smaller energy gap of 7.35 eV. This agrees well with the result obtained by the surface sensitive EELS experiment (7.4 eV, see Figure 4).

For the investigation of the influence of additional polarization and diffuse atomic basis functions we performed calculations of the electronic end energetic properties of  $\text{MgSO}_4$ ,  $\text{MgSO}_4 \cdot \text{H}_2\text{O}$ , and the (100) surface of  $\text{MgSO}_4 \cdot \text{H}_2\text{O}$ . In this case the 6-31G\*, 6-311+G\*, 6-311+G\*\*, and 6-311+G\*\*(2p2d) basis sets were used for water together with an additional d orbital for Mg, S, and O atoms of the mineral. Our calculations show that there are only small changes of the shape of the bands. The calculated value of the band gap changes by only  $\pm 0.15$  eV for the surface and by  $\pm 0.05$  eV for the bulk (see Table 3). Further extension of the basis set of the Mg, S, and O atoms with diffuse sp orbitals leads to severe SCF convergence problems for  $\text{MgSO}_4$  and the surface of  $\text{MgSO}_4 \cdot \text{H}_2\text{O}$ . The variation of total energies obtained with different basis sets is also small and does not exceed 0.13 eV per atom.

**TABLE 3: Band Gap of the  $\text{MgSO}_4 \cdot \text{H}_2\text{O}$  and Surface of the  $\text{MgSO}_4 \cdot \text{H}_2\text{O}$  Obtained with Different Basis Sets**

	basis set <sup>a</sup>	band gap (eV)
$\text{MgSO}_4 \cdot \text{H}_2\text{O}$	6-31G*	7.77
	6-31G* + d	7.74
	6-311+G**	7.81
	6-311+G**(2p2d)	7.82
	6-311+G** + d	7.81
surface of $\text{MgSO}_4 \cdot \text{H}_2\text{O}$	6-31G*	7.35
	6-311+G**	7.20
	6-311+G**(2p2d)	7.32

<sup>a</sup> Here “+ d” means that additional d orbital was added for the basis sets of Mg, S, and O atoms.

### V. Adsorption of the Single Water Molecules on $\text{MgSO}_4 \cdot \text{H}_2\text{O}$

To investigate both the chemical influence of the  $\text{MgSO}_4 \cdot \text{H}_2\text{O}$  surface and possible changes in the surface band structure due to molecular adsorption, the calculations were extended to include the adsorption of single water molecules. The energetically favored positions were calculated using MSINDO CCM. As mentioned above, only the atoms of topmost 7 atomic layers were allowed to relax. To investigate the most stable adsorption site, the  $\text{H}_2\text{O}$  molecule was placed at  $14 \times 14$  different surface sites within the unit cell. At each of these points, the adsorption energy  $E_{\text{ads}}$  was calculated including relaxation of both the molecule and the surface.

$$E_{\text{ads}} = E(\text{H}_2\text{O}/\text{MgSO}_4 \cdot \text{H}_2\text{O}) - E(\text{MgSO}_4 \cdot \text{H}_2\text{O}) - E(\text{H}_2\text{O})$$

A negative adsorption energy indicates a stable adsorption position. As examples, three configurations are shown in Figure 6. For these positions,  $E_{\text{ads}}$  is  $-0.05$  eV (a),  $-0.61$  eV (b), and  $-1.20$  eV (c). The geometry shown in Figure 6 c is energetically the most favorable found by our calculations.

As expected, the site above a surface Mg atom (6c) is preferred for water adsorption due to the interaction between the electropositive Mg atom and the electronegative O atom of the water molecule. This configuration is stabilized by two additional hydrogen bonds between the H atoms of the water and the O atoms of the  $\text{SO}_4$  units. The energy difference between the hydrogen bond and the  $\text{Mg}-\text{O}_{\text{H}_2\text{O}}$  bond is approximately 0.6 eV. The length of the  $\text{Mg}-\text{O}_{\text{H}_2\text{O}}$  bond is 2.18 Å.

The electronic density of states for two energetically favorable types of bonds was calculated with the PW1PW method. The results of the calculations are presented in Figure 7. Compared to the spectrum of the clean surface (cf. with Figure 5c), the

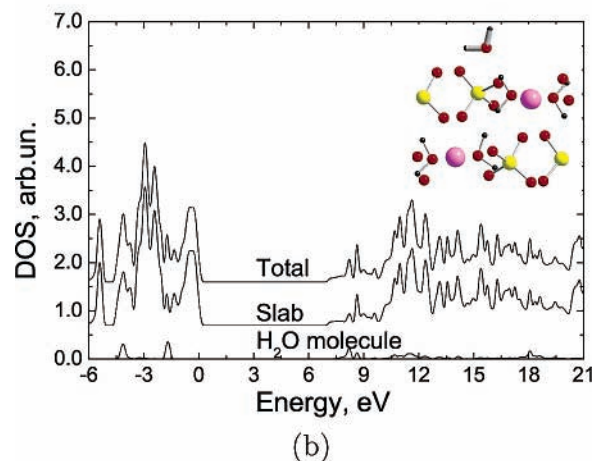
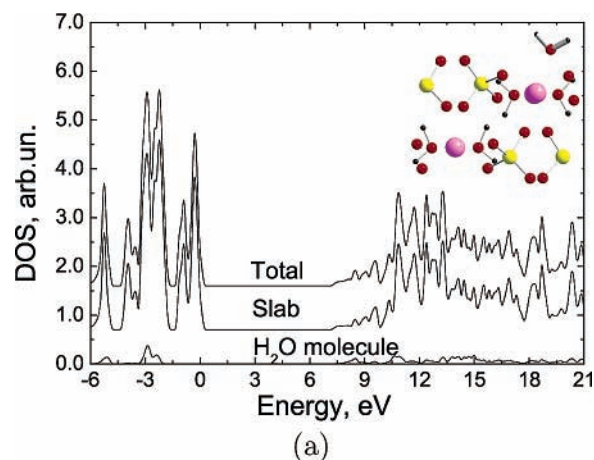


**Figure 7.** Calculated density of states of two most stable positions of a single water molecule adsorbed on the  $\text{MgSO}_4 \cdot \text{H}_2\text{O}$  surface: (a) water molecule above Mg position (see Figure 6c) and (b) above S atom (cf. with Figure 6b); PW1PW results using optimized structures obtained with MSINDO.

chemisorbed water molecule increases slightly the density of the unoccupied states. The first occupied state of the molecular water ( $1b_1$  state) is around 3 eV below the valence band edge of the  $\text{MgSO}_4 \cdot \text{H}_2\text{O}$  surface. Similar results for molecularly adsorbed water on insulating surfaces were found by previous UPS measurements of  $\text{H}_2\text{O}$  on  $\text{NaCl}(100)$  and  $\text{KCl}(100)$ .<sup>31</sup> From Figure 7 an overlap of the  $\text{O}2p$  orbital of the water molecule with the valence band structure stemming from the O atoms around the  $\text{SO}_4$  units can be seen. In analogy to the results

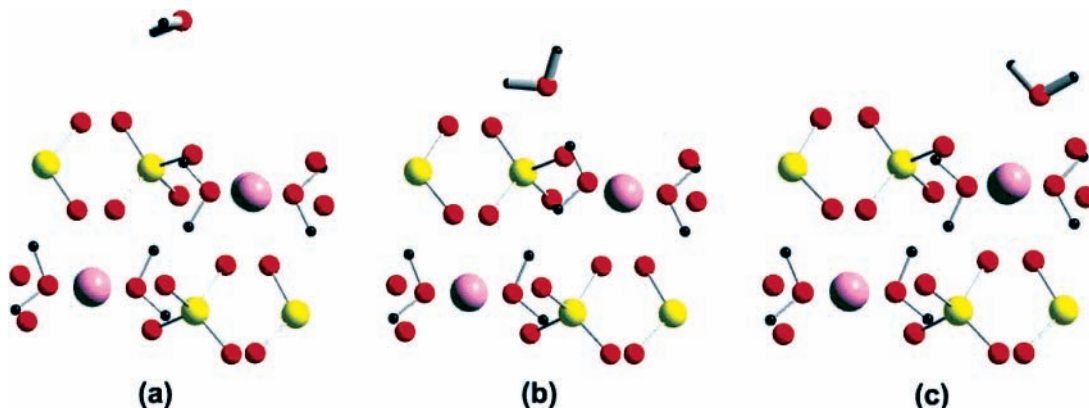


**Figure 6.** Three minimum structures for molecular water adsorption on  $\text{MgSO}_4 \cdot \text{H}_2\text{O}$  (100), as obtained with MSINDO. In structure (a) the water molecule is attached to the surface via two hydrogen bonds to surface oxygens, in structure (b) one hydrogen bond between water oxygen and surface hydrogen is formed, and in (c) water interacts with surface Mg and oxygen.



obtained for bulk  $\text{MgSO}_4 \cdot \text{H}_2\text{O}$ , the  $\text{Mg}-\text{O}_{\text{H}_2\text{O}}$  bond between the surface Mg atom and the O atom of the adsorbed water molecule is mainly electrostatic, i.e., only polarization effects of the polar bond can be seen in the DOS spectrum by both small energetic shifts and intensity changes.

It was found that the slab with the adsorbed molecule has a dipole moment of 3.4 D in the direction of the surface normal. To investigate the influence of the induced artificial dipole moment we repeated the calculation of the electronic properties of the slab with adsorbed water molecules at both sides. The energetically favorable position of  $\text{H}_2\text{O}$  on the surface as described above was used for the investigation. The thickness of the slab was increased to 21 atomic layers, which reduces the interaction between adsorbed  $\text{H}_2\text{O}$  molecules. After relaxation the total dipole moment of the slab with two molecules was zero. The band structure calculations show that the shape of the bands are practically the same as for the one-side adsorption. The change of the band gap is only 0.05 eV. Moreover, the geometry of adsorbed water molecules for symmetrical and asymmetrical slab are the same. The bond distance between adsorbed water and the surface ( $\text{O}_{\text{water}}-\text{Mg}_{\text{slab}}$ ) are the same, 2.1 Å. Note that the slab itself does not have a dipole moment, thus there are no dipole-dipole interactions between water and the surface.

According to our present results, water adsorption on the surface of the  $\text{MgSO}_4 \cdot \text{H}_2\text{O}$  crystal does not change the band gap and induces only small changes in the overall DOS. This makes it experimentally difficult to distinguish between water molecules belonging either to the bulk or to the surface. An impact of the interaction between the water molecule and the surface can be seen only for metastable adsorption sites (see Figure 7b). The most intense peak in the DOS spectrum is shifted by about 0.3 eV to higher binding energies as a consequence of the stronger interaction between the O of the water molecule with the O atoms of the  $\text{SO}_4$  unit of the underlying surface. The attractive interaction between the water and the S atom causes changes in the density of the unoccupied states.

## VI. Summary and Conclusions

In this paper, we have shown first theoretical results about both the geometric and electronic structure of  $\text{MgSO}_4 \cdot \text{H}_2\text{O}$  and  $\text{MgSO}_4$ . The focus was on surface properties of  $\text{MgSO}_4 \cdot \text{H}_2\text{O}$  and the adsorption of water. For the calculation of electronic properties a combination of two theoretical models was applied, the HF-DFT hybrid approach PWIPW and the semiempirical method MSINDO. For both methods the calculated bulk structure parameters of  $\text{MgSO}_4$  and  $\text{MgSO}_4 \cdot \text{H}_2\text{O}$  are in good agreement with experimental data. Using the hybrid method PWIPW the band gap can be calculated accurately for the surface structure of  $\text{MgSO}_4 \cdot \text{H}_2\text{O}$ . This was demonstrated by comparison to our EELS measurement for polycrystalline kieserite minerals. For a complete scan of the potential surface for water adsorption on  $\text{MgSO}_4 \cdot \text{H}_2\text{O}$  surface, the semiempirical MSINDO method proved to be useful. Electronic structure calculations with PWIPW based on the optimal adsorption structures found with MSINDO calculations have shown that both the chemically combined water inside the crystal and also water molecules adsorbed on top of the surface leave the electronic structure near the band edges almost unchanged. The

valence band is generated mostly by the 2p orbitals of the O atoms of the  $\text{SO}_4$  units, whereas the conduction band is formed by the 2p states of the S atoms. The oxidation state of the Mg atoms is close to +2. Therefore, covalent bonds between the Mg atoms and the  $\text{SO}_4$  molecules are not present. This can explain why also the chemisorbed water molecule at Mg surface sites does not change either the conduction nor the valence band edge, which is an important observation for any kind of chemical reactions, as seen for the adsorption of salicylic acid on the  $\text{MgSO}_4 \cdot \text{H}_2\text{O}$  surface.<sup>27</sup>

**Acknowledgment.** The financial support of this project by the K+S and the DAAD is gratefully acknowledged.

## References and Notes

- (1) Henrich, V. E.; Cox, P. A. *The Surface Science of Metal Oxides*; Cambridge University Press: Cambridge, 1996.
- (2) Over, H.; Kim, Y. D.; Seitsonen, H. P.; Wendt, S.; Lundgren, E.; Schmid, M.; Varga, P.; Morgante, A.; Ertl, G. *Science* **2000**, *287*, 1474.
- (3) Knözinger, E.; Sterrer, M.; Diwald, O. *J. Mol. Catal. A Chemical* **2000**, *162*, 83.
- (4) Diwald, O.; Berger, T.; Sterrer, M.; Knözinger, E. *Stud. Surf. Sci. Catal.* **2001**, *140*, 237.
- (5) Brockhoff, A. *Kali und Steinsalz* **2003**, *1*, 42.
- (6) Tegenkamp, C.; Pfnür, H. *Phys. Chem. Chem. Phys.* **2002**, *4*, 2653.
- (7) Bredow, T.; Gerson, A. R. *Phys. Rev. B* **2000**, *61*, 5194.
- (8) Perdew, J. P.; Wang, Y. *Phys. Rev. B* **1992**, *45*, 13244.
- (9) Saunders, V. R.; Dovesi, R.; Roetti, C.; Orlando, R.; Zicovich-Wilson, C. M.; Harrison, N. M.; Doll, K.; Civalieri, B.; Bush, I.; D'Arco, Ph.; Llunell, M. *CRYSTAL2003 User's Manual*; University of Torino: Torino, 2003.
- (10) McCarthy, M. I.; Harrison, N. M. *Phys. Rev. B* **1994**, *49*, 8574.
- (11) Towler, M. D.; Harrison, N. M.; McCarthy, M. I. *Phys. Rev. B* **1995**, *52*, 5375.
- (12) [http://www.crystal.unito.it/Basis\\_Sets/sulphur.html](http://www.crystal.unito.it/Basis_Sets/sulphur.html).
- (13) Hehre, W. J.; Ditchfield, R.; Pople, J. A. *J. Chem. Phys.* **1972**, *56*, 2257.
- (14) Monkhorst, H. J.; Pack, J. D. *Phys. Rev. B* **1976**, *13*, 5188.
- (15) Ahlswede, B.; Jug, K. *J. Comput. Chem.* **1998**, *20*, 563.
- (16) Ahlswede, B.; Jug, K. *J. Comput. Chem.* **1998**, *20*, 572.
- (17) Nanda, D. N.; Jug, K. *Theor. Chem. Acta* **1980**, *57*, 93.
- (18) Bacon, A. D.; Zerner, M. C. *Theor. Chem. Acta* **1979**, *53*, 21.
- (19) Jug, K.; Bredow, T. SINDO1, in *Encyclopedia of Computational Chemistry*; Schleyer, P. v. R., Allinger, N. L., Clark, T., Gasteiger, J., Kollman, P. A., Schaefer, H. F., III, Schreiner, P. R., Eds.; Wiley: New York 1998; Vol. 4, p 2599.
- (20) Bredow, T.; Jug, K. MSINDO, in *Encyclopedia of Computational Chemistry* (online edition); Schleyer, P. v. R., Schaefer, H. F., III, Schreiner, P. R., Jorgensen, W. L., Thiel, W., Glen, R. C., Eds.; John Wiley & Sons Ltd.: Chichester, UK, 2004. DOI: 10.1002/0470845015.cu0001.
- (21) Janetzko, J.; Bredow, T.; Jug, K. *J. Chem. Phys.* **2002**, *116*, 8994.
- (22) Bredow, T.; Geudtner, G.; Jug, K. *J. Comput. Chem.* **2001**, *22*, 861.
- (23) Jug, K.; Bredow, T. *J. Comput. Chem.* **2004**, *25*, 1551.
- (24) Rentzeperis, P. J.; Soldatos, C. T. *Acta Crystallogr.* **1958**, *11*, 686.
- (25) Bregeault, J. M.; Herpin, P.; Manoli, J. M.; Pannetier, G. *Bull. Soc. Chim. Fr.* **1970**, 4243.
- (26) Vogt, J.; Weiss, H. *Surf. Sci.* **2001**, *491*, 155.
- (27) Kovalev, O. V. *Representations of the Crystallographic Space Groups: Irreducible Representations, Induced Representations, and Corepresentations*; Gordon and Breach: Philadelphia, 1993.
- (28) Tegenkamp, C.; Pfnür, H.; Ernst, W.; Malaske, U.; Wollschläger, J.; Peterka, D.; Schröder, K. M.; Zielasek, V.; Henzler, M. *J. Phys.: Condens. Matter* **1999**, *11*, 9943.
- (29) Maslyuk, V. V.; Tegenkamp, C.; Bredow, T.; Pfnür, H. *Adsorption of benzoic acid and its OH-substituted derivatives on kieserite*, in preparation.
- (30) Pisani, C.; Dovesi, R.; Roetti, C. *Hartree-Fock ab initio Treatment of Crystalline Systems*; Lecture Notes in Chemistry; Springer-Verlag: Heidelberg, 1988; Volume 48.
- (31) Broqvist, P.; Gronbeck, H.; Panas, I. *Surf. Sci.* **2004**, *554*, 262.
- (32) Schintke, S.; Schneider, W. D. *J. Phys.: Condens. Matter* **2004**, *16*, R49.
- (33) Fölsch, S.; Henzler, M. *Surf. Sci.* **1991**, *247*, 269.